Superconducting Cavity Design for the International Linear Collider

A. Kabel*, V. Akcelik, A. Candel, L. Ge, K. Ko, L. Lee, Z. Li, C. Ng,
E. Prudencio, G. Schussman, R. Uplenchvar, L. Xiao,
SLAC, Menlo Park, CA 94025, U. S. A.

Abstract

Over the past years, SLAC's Advanced Computations Department (ACD), under SciDAC sponsorship, has developed a comprehensive portfolio of advanced parallel electromagnetic simulation tools comprising, among others, the codes **Omega3P** (eigensolver), **T3P** (wakefields), **Track3P** (multipacting), and **S3P** (scattering matrix), all utilizing a common framework for the Finite Element Method in electromagnetics. Using these codes, a large part of ACD's efforts has addressed simulation studies for the International Linear Collider (ILC). We give typical examples of simulation results from this area, highlighting code capabilities.

INTRODUCTION

The United States' Department of Energy (DOE), through its Office of Science, is promoting the use of High-Performance Computing in its mission-relevant projects. The 'Scientific Discovery through Advanced Computation' (SciDAC) program has, since its inception in 2001, been funding efforts at SLAC to develop a high-performance, massively parallel electromagnetic (EM) modeling capability for the use in the operation of current and the design of future accelerator facilities [1, 4].

Unlike other software typically used in electromagnetic modeling in accelerator physics, the program at SLAC makes use of the Finite-Element Method (FEM). The FEM allows for conformal modeling of smoothly curved boundaries; a cell in the FEM can support degrees of freedom for higher-order polynomial functions, resulting in high accuracy for relatively small numbers of grid points.

Another distinguishing feature of the SLAC EM codes is the massively parallel use of resources, both CPU time and memory. To our knowledge, no other FEM code in use in electromagnetic modeling can make use of the superior capability of supercomputers; thus, other codes face limitations when modeling large-scale accelerator systems.

The code suite developed at SLAC over the past years comprises

- **Omega3P**—a complex-domain eigensolver for finding normal modes and their frequencies and damping factors in radio-frequency (RF) cavities,
- **S3P**—a frequency-domain code to determine scattering matrix elements of RF structures,
- **T3P**—a time-domain solver calculating transient behavior of electromagnetic fields in RF cavities driven by particle currents and external fields, and
- **Track3P**—a tracking code for particles in RF cavities; it is used for calculating such effects as multipacting and dark currents.

The codes

- **Pic3P**—a particle-in-cell code for RF guns and Klystrons, and
- **Gun3P**—a static solver with particles for calculating the formation and transport of direct-current beams

are currently under development.

All codes are based on a common framework of tetrahedral, finite-element grids. The codes have been successfully applied to a variety of problems in accelerator physics, including, but not limited to, the Next Linear Collider project and SLAC's PEP-II and LCLS facilities. Recently, we have invested considerable effort to applying these codes to problems connected to the International Linear Collider (ILC) project. In the following, we will present some of these applications as well as typical results.

THE ILC TDR CAVITY

The temporal electromagnetic field behavior in the ILC baseline TDR (TESLA) cavity due to a beam transit was simulated with **T3P** to obtain useful information on the transients in the cavity and the 3D effects from the couplers (input and HOM) on the short range wakefields. Figs. 1 shows two snapshots in time of the magnetic fields (image current) on the cavity wall induced by the transiting beam: the first set of pictures from before the beam enters the cavity and the second set after the beam has passed. Performed on the DOE's National Energy Research Scientific Computing Center's (NERSC) 'Seaborg' supercomputer, the **T3P** simulation used 1.75 million quadratic elements (10^7 DOFs) requiring 173GB of memory on 1024 CPUs and 47 minutes of CPU time per nano-second of beam travel.

In the frequency domain, results obtained from simulation can be readily compared with data available for the measured TESLA TDR cavities. For this kind of study, high accuracy in determining frequency and quality factor is imperative. Figs. 2 and 3 demonstrate the suitability of the FEM for this purpose; increasing the element order leads to a rapidly decreasing frequency error.

*andreas.kabel@slac.stanford.edu

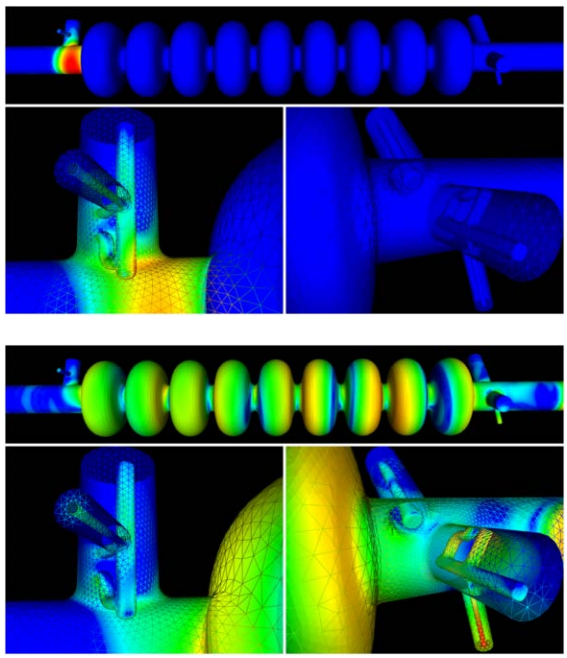

Figure 1: Snapshots of **T3P** magnetic field contours on the wall surface of the TDR cavity and couplers before beam enters main cavity (top) and after exiting output end beampipe (bottom).

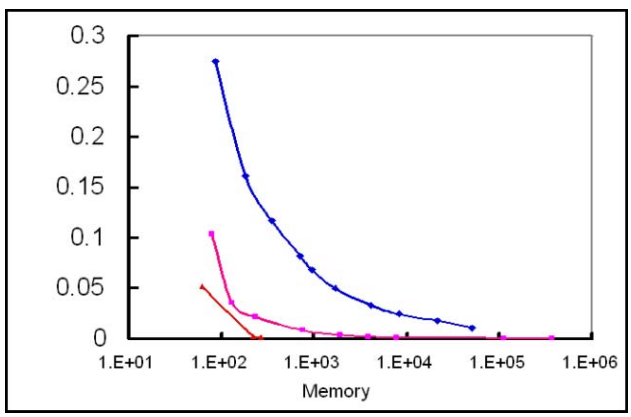

Figure 2: Frequency convergence: relative error in % vs. memory requirements for different order of FEs (blue: $p = 1$; magenta: $p = 2$, red: $p = 3$)

Still, the high memory requirements even for quadratic elements necessitates the use of parallelism for capability reasons alone. As an attractive side-feature, the parallelization will also bring down the run-time of a simulation.

We have done a series of calculations of ω and Q_{ext} for the TESLA TDR cavities. As the dipole mode degeneracy is split by the symmetry-breaking input and higher-order mode (HOM) couplers, each of the two dipole bands in the TDR cavity consists of nine pairs of modes. Fig. 4 shows the comparison between the **Omega3P** results for the ideal cavity and the measurement of eight cavities in a DESY

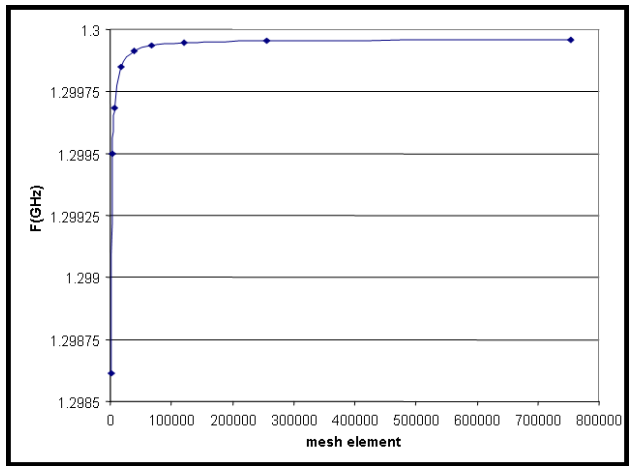

Figure 3: Frequency convergence vs. number of mesh-points for $p = 2$ for different order of FEs (blue: $p = 1$; magenta: $p = 2$, red: $p = 3$)

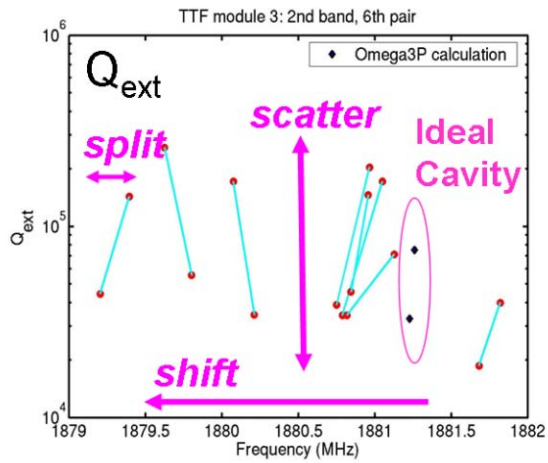

Figure 4: Comparison between ideal cavity results from **Omega3P** and measurements from eight different TESLA cavities in an actual cryomodule, showing differences in mode splitting, mode frequencies, and damping.

cryomodule for the sixth pair in the second band. We observe that for the measured data:

1. the splitting of the mode pair is larger,
2. the mode pair is mostly shifted to lower frequencies,
3. and their Q_{ext}'s are scattered towards the high side.

The Q_{ext} increase would be problematic if it leads to Q_{ext} exceeding the beam stability limit.

The differences between simulation and measurement can be attributed to cavity deformations. We have started an effort to determine the cavity shape by solving an inverse problem using the TESLA data as input parameters [3]. The problem is formulated as a least-squares minimization problem using typical deformation parameters as its

variables; it is solved using a reduced-space Gauss-Newton method. We have been able to successfully reproduce the deformation of an artificially distorted cavity simulation by looking at its ω, Q spectrum. Work on the actual TDR cavities is in progress.

An interesting phenomenon was discovered in these numerical simulations: A pair of planar polarized waves can turn into a pair of elliptically polarized modes: if its degeneracy is split by asymmetry and the finite-width spectral lines overlap (due to external or natural damping). Viewed at a fixed point, the temporal behavior of a rotating dipole wake will be a $\vec{E}$ vector rotating on an ellipse.

This eigenmode will lead to an intrinsic x-y-coupling due to transverse wakes; as opposed to coupling introduced by a mere rotation of a planar mode, this coupling is independent of the orientation of the cavity. From a beam-dynamics viewpoint, this requires the augmentation of standard wake formulations in tracking codes by relative-orientation dependent, or matrix-valued, kick strengths.

LOW-LOSS CAVITY

The Low-Loss cavity design [2] (Fig. 5) is being considered as a possible alternative to the baseline TDR cavity for the ILC main linac. Based on a different cell shape, its cryogenic losses would be 20% lower than the baseline design; also, it would achieve a higher gradient by using a smaller cavity iris. Additionally, the endpipes where the couplers are located are larger than the cavity iris to allow for adequate coupling to the input coupler and more effective HOM damping. Using the HOM coupler from the TESLA cavity directly, **Omega3P** analysis found that the first mode in the third dipole band does not meet a beam stability requirement of $Q_{ext} < 10^5$.

A high-fidelity mesh consisting of 530,000 quadratic elements (3.5 million degrees of freedom (DOFs)) was used to model the cavity. This provides sufficient resolution for modifying the end groups to improve the HOM damping. By adjusting the end-pipe radius, the HOM coupler azimuthal location, and the loop shape and configuration (Fig. 5, colored inserts), the Q_{ext} of the dangerous third band mode was reduced to below the stability threshold. The **Omega3P** simulations were performed on NERSC's Seaborg and Bassi clusters as well as on NCCS's Phoenix machine. A comparison between the original and the new damping results is shown in Fig. 6.

CRAB CAVITY

The crab cavity is a design option for an ILC with a non-zero crossing angle at the interaction point. It is an RF cavity which using its first deflecting mode to rotate the beam bunches to achieve head-on collisions and thus higher luminosity at the ILC interaction point. The existing FNAL design has been simulated and preliminary modifications have been made to the computational model (Fig. 7) to provide improved damping results (Fig. 8).

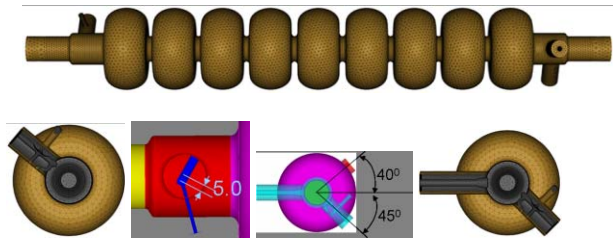

Figure 5: Mesh models of the low-loss cavity including the endgroups and with the modifications of the HOM loop orientation and the coupler location shown in colored inserts.

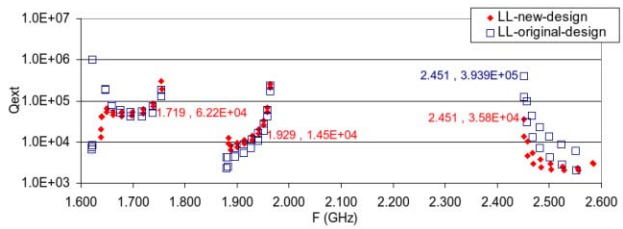

Figure 6: Q_{ext} versus frequency for the low-loss cavity with TESLA HOM coupler (in blue) and SLAC's improved design (in red).

MULTIPACTING AND NOTCH FILTER SENSITIVITY IN THE ILC 'ICHIRO' CAVITY

Researchers at KEK are devoting considerable effort to developing a high-gradient cavity for the ILC, focussing on the so-called 'ICHIRO' cavity [5] which evolved from the Low-Loss cavity design described above. The ICHIRO cavity differs from the Low-Loss design in the enlarged end-tube at the input end.

In single-cell tests, the ICHIRO design has established a record gradient of 54MV/m; 9-cell ICHIRO cavities, how-

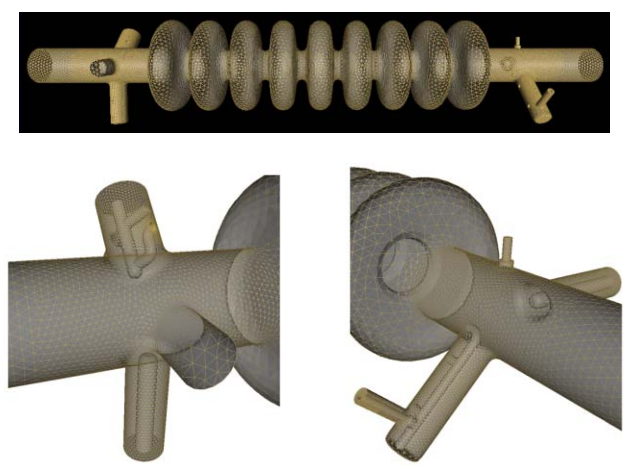

Figure 7: Mesh model of the FNAL design of the ILC crab cavity showing input, LOM, SOM and HOM couplers.

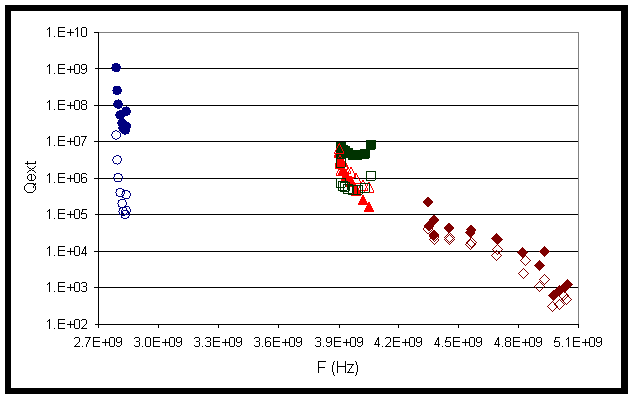

Figure 8: Mode damping improvements in the ILC crab cavity after first SLAC modifications. Solid markers: Original FNAL design, Hollow markers: with SLAC improvements. Blue: first monopole band, green: y-polarized first dipole band, red: x-polarized first dipole band, maroon: second dipole band.

Figure 9: 9-cell ICHIRO cavity prototype under high power tests at KEK with enlarged end-tube shown on the input end to the left

ever, (Fig. 9) are having difficulties reaching gradients surpassing 30 MV/m.

Using the tracking code **Track3P**, multipacting activity in the transition from the enlarged end-tube to the beampipe was observed in simulations (Fig. 9). The calculated multipacting levels are found to be in good agreement with experimental results, at KEK, for X-ray barriers (Fig. 10). Work is underway to redesign the cavity to mitigate or circumvent this problem.

The notch filter in the TESLA HOM coupler used in the Ichiro cavity is designed to reject the fundamental mode power while allowing damping of all higher-order modes. To study its sensitivity and detuning effect due to a change in notch gap dimensions, two calculations were carried out.

First, the tuning curves of the HOM coupler for three different notch gap dimensions were computed with **S3P** to find the filter's response around the fundamental mode frequency of 1.3 GHz (Fig. 11, center), and a sensitivity of 0.11 MHz per micron was obtained. Next, the fundamental mode was computed for the cavity complete with HOM couplers set at the three different notch gap dimensions. A comparison of the fields in the HOM couplers from the fundamental mode in the three cases is shown in the table in Fig. 11, bottom. While the notch gap fields vary little in all cases, the Q_{ext} of the mode is reduced by orders of magnitude when the notch filter is tuned far off the notch

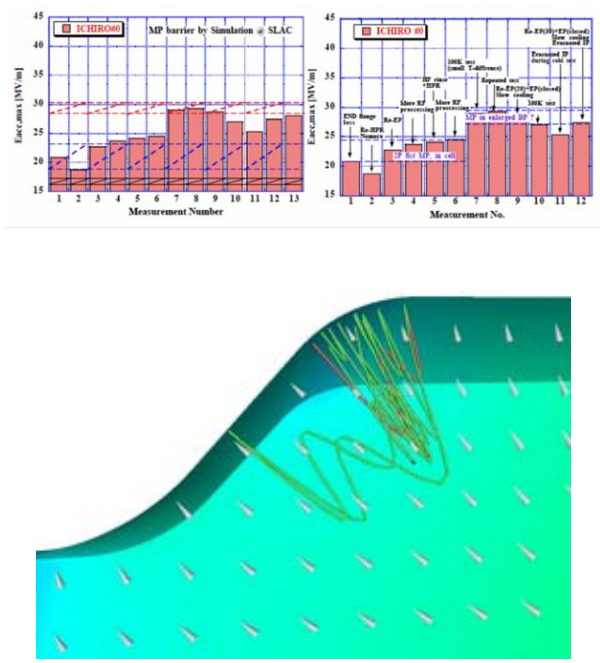

Figure 10: (Top Left) MP barriers in 9-cell ICHIRO cavity calculated with Track3P, (Top Right) MP barriers measured on ICHIRO prototype (courtesy K. Saito, KEK). (Bottom) Typical trajectory for a multipacting process obtained from **Track3P**

frequency at 1.3 GHz. This could lead to large amounts of power flowing through the feed-through and might result in excessive heating if proper cooling is not factored into the design.

MULTIPACTING IN THE TTF INPUT COUPLE

Track3P simulations are being performed to investigate the effect of multipacting on the processing of the ILC TTF III input coupler. A model of the coupler is shown in Fig. 12 (top). Initial studies have been focusing on the region around the cold bellows as depicted in light blue in the model. The operating power level is between 300kW and 400kW. Simulations exhibit multipacting activity near a power level of 360kW, with multipacting particles impacting the outer wall of the coaxial, but no impacts within the bellows. The distribution of impact particles shown in Fig. 12 (center) reflects the electric field profile along the coaxial, which has a standing wave component—caused by a slight mismatch of the bellows in our model—on the upstream side of the bellows but remains a purely traveling wave on the downstream side. A typical particle trajectory on the upstream side is displayed in Fig. 12 (Bottom); it represents a fifth-order multipacting process. The simulation will be extended to include the entire coupler geometry.

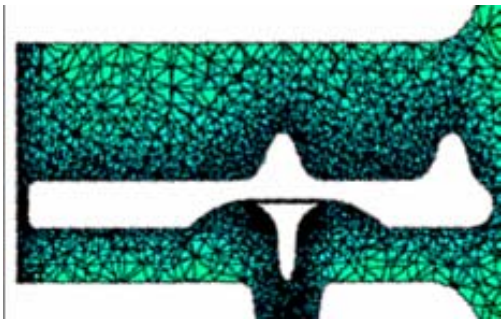

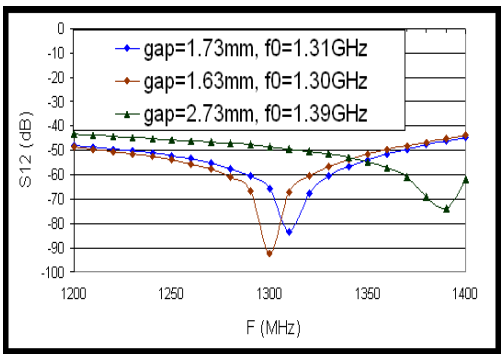

Notch gap (mm)	Notch gap field (MV/m)		Antenna tip Field (MV/m)		Qext of HOM port @1.3GHz	
	Up-stream	Down-stream	Up-stream	Down-stream	Up-stream	Down-stream
1.63	16.9	5.0	0.8	0.2	6.1e+9	1e+12
1.73	16.5	4.9	1.4	0.4	5.2e+8	9.e+9
2.73	13.3	3.9	6.1	3.0	1.4e+7	1.7e+8

Figure 11: (Top) Detailed mesh in the ICHIRO HOM coupler showing mesh density in the notch gap and near the antenna tip, (Middle) tuning curves of HOM coupler with three different notch gaps near 1.3GHz, (Bottom) Field values in the notch gap and at the antenna tip for three different notch gap dimensions and the corresponding Q_{ext}.

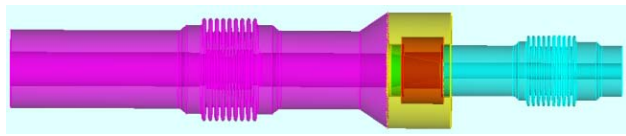

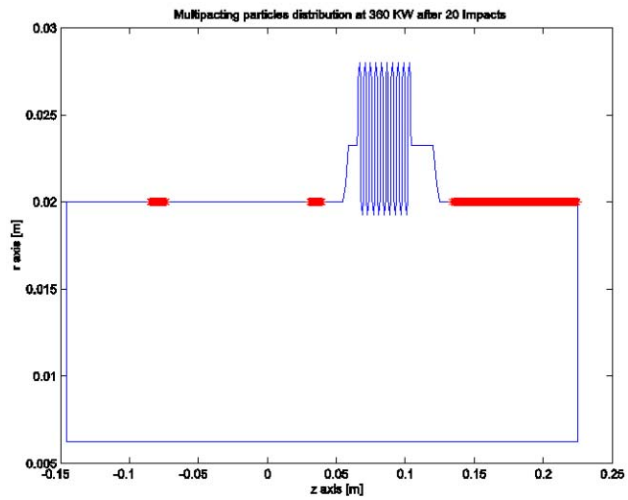

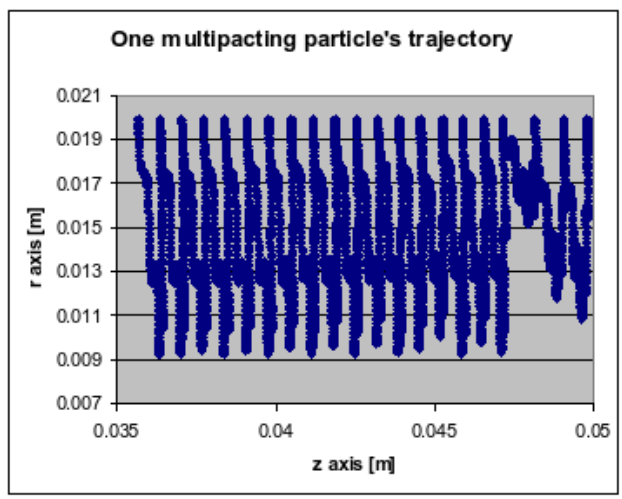

Figure 12: (Top) Model of the TTF III input coupler, (Middle) impacts of multipacting particles along the outer wall of coax, (Bottom) a typical particle trajectory with impacts close to the cold bellows on the upstream side.

ILC MULTI-CAVITY STRUCTURES

The superstructure design for the ILC combines two or more cavities through weakly coupled beampipes into a single unit. First studied at DESY, the goal of this arrangement is to reduce the number of input couplers and increase the packing factor to reduce linac length. A concern with superstructures is the possible presence of trapped EM modes between cavities. Fig. 13 shows an example of a two-cavity superstructure model and a HOM trapped between the cavities, as computed by **Omega3P**.

The ILC Global Design Effort has expressed strong interest in computing the wakefields for an ILC RF unit comprising three cryomodules with eight TDR cavities each. As a first step toward this goal, a four-cavity structure (relevant to KEK's STF cryomodule), has been modeled using the DOE's National Leadership Computing Facility's (NLCF) 'Phoenix' machine.

The solution method used was Second-Order Arnoldi with restarted Generalized Minimal Residual Method and a multi-level preconditioner. One of the modes with high fields in between the cavities obtained in these calculation is shown in Fig. 14.

A rough estimate of the computational requirements for modeling the entire ILC RF unit yields $\approx 2 \cdot 10^7$ quadratic elements ($\approx 10^8$ DOFs) and several thousand modes. Simulations of this magnitude will be extremely challenging and will require peta-scale computing resources as well as advances in scalable eigensolver algorithms and parallel refinement techniques. Efforts in these two computational science research areas are in progress under the SciDAC project.

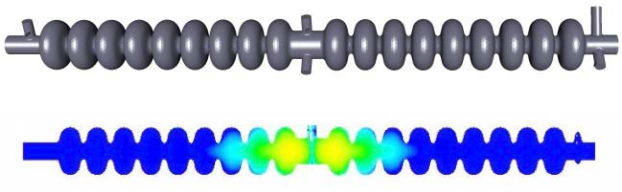

Figure 13: Two-cavity superstructure model (top) and a trapped mode found by **Omega3P** (bottom).

ACKNOWLEDGEMENTS

This work was supported by U. S. A. DOE contract DE-AC-002-76SF00515. This research used resources of the National Energy Research Scientific Computing Center, which is supported by the Office of Science of the U. S. Department of Energy under Contract No. DE-AC02-05CH11231; and of the National Center for Computational Sciences at Oak Ridge National Laboratory, which is supported by the Office of Science of the U. S. Department of Energy under Contract No. DE-AC05-00OR22725. – We thank C. Adolphsen, T. Higo, K. Saito, and J. Sekutowicz for valuable input. We also acknowledge the contributions from our SciDAC collaborators in numerous areas of computational science.

REFERENCES

[1] K. Ko et al., SciDAC and the International Linear Collider: Petascale Computing for Terascale Accelerator; Invited Talk given at SciDAC 2006 Conference, Denver, Colorado, June 25–29, 2006

[2] J. Sekutowicz et al., Design of a Low Loss SRF Cavity for the ILC, Proc. PAC 2005, Knoxville, Tennessee, May 12–16, 2005

[3] V. Akcelik et al., Adjoint Methods for Electromegnetic Shape Optimization of the Low-Loss Cavity for the International Linear Collider; Proc. SciDAC Conference, San Francisco, California, 2005

[4] K. Ko et al., Advances in Electromagnetic Modeling through High-Performance Computing; Proc. SRF Workshop 2005, Cornell University, July 10–15, 2005

[5] T. Saeki et al., Fabrication of Four 9-Cell Ichiro High-Gradient Cavities for the R&D of ILC Accelerator in KEK; ; Proc. SRF Workshop 2005, Cornell University, July 10–15, 2005

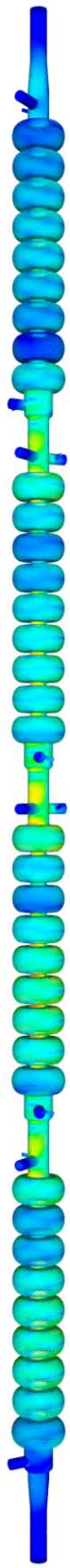

Figure 14: One **Omega3P** computed HOM in the ILC 4-cavity structure with strong fields between cavities.